Polyhedron xxx (2012) xxx–xxx

Contents lists available at SciVerse ScienceDirect

Polyhedron

journal homepage: www.elsevier.com/locate/poly

Reactions of a tungsten alkylidyne complex with mono-dentate phosphines: Thermodynamic and theoretical studies

Ping Chen [a], Brenda A. Dougan [b], Xinhao Zhang [a,*], Yun-Dong Wu [a,*], Zi-Ling Xue [b,*]

[a] Lab of Computational Chemistry and Drug Design, Laboratory of Chemical Genomics, Peking University Shenzhen Graduate School, Shenzhen 518055, PR China
[b] Department of Chemistry, University of Tennessee, Knoxville, TN 37996, USA

ARTICLE INFO

Article history:
Available online xxxx

Dedicated to the memory of Michelle Millar, a scientist and teacher who gave so much to the chemistry communities.

Keywords:
Alkylidyne
Alkylidene
Phosphine adduct
Equilibrium
DFT calculations
α-H abstraction

ABSTRACT

Addition of mono-dentate phosphines PMe_3 and PMe_2Ph to the W(VI) alkyl alkylidyne complex $W(CH_2SiMe_3)_3(\equiv CSiMe_3)$ (**1**) is reversible, each reaching equilibrium. Thermodynamic studies of the equilibria have been conducted, giving $\Delta H^\circ = -10.0(1.1)$ kcal/mol and $\Delta S^\circ = -23(4)$ eu for the addition of PMe_3 and $\Delta H^{\circ\prime} = -3.0\ (0.7)$ kcal mol^{-1} and $\Delta S^{\circ\prime} = -6(3)$ eu for the addition of PMe_2Ph, indicating that the addition is exothermic. The experimental measurement allows a benchmarking study to select a proper DFT method to describe the current system. Of the DFT methods tested, M06 has demonstrated superior performance in calculating binding energy of a bimolecular reaction. The calculated reaction pathways show that $W(CH_2SiMe_3)_3(\equiv CSiMe_3)$ (**1**) reacts with PR_3 to form $W(CH_2SiMe_3)_3(\equiv CSiMe_3)(PR_3)$ ($PR_3 = PMe_3$, **3a**; PMe_2Ph, **3b**), and the adduct then undergoes α-H migration to form $W(CH_2SiMe_3)_2(=CHSiMe_3)_2(PR_3)$ (**4a**, **4b**). **4a** and **4b** are found to be thermodynamically and kinetically stable intermediates. The calculations also suggest a pathway in the formation of the alkyl alkylidene alkylidyne complex $W(CH_2SiMe_3)(=CHSiMe_3)(\equiv CSiMe_3)(PR_3)_2$ (**5a**).

1. Introduction

High-oxidation-state metal alkylidene and alkylidyne complexes containing M=C and M≡C bonds, respectively, often demonstrate unique chemistry and have been extensively studied [1–4]. The alkylidene and alkylidyne complexes usually contain ligands such as neopentyl ($-CH_2CMe_3$) and trimethylsilylmethyl ligands ($-CH_2SiMe_3$) that are free of β-H atoms [1–4]. Complexes containing a $-CH_2SiMe_3$ ligand with a β-Si atom often show properties different from those containing its neopentyl $-CH_2CMe_3$ analog. For example, Clark and Schrock reported that the reactions of $W(CH_2CMe_3)_3(\equiv CCMe_3)$ with phosphines PMe_3 and $Me_2PCH_2CH_2PMe_2$ (DMPE) give the bis-phosphine/chelating phosphine products $W(CH_2CMe_3)(=CHCMe_3)(\equiv CCMe_3)(PMe_3)_2$ and $W(CH_2CMe_3)(=CHCMe_3)(\equiv CCMe_3)$(DMPE) through α-H abstraction [3b]. The structure of the latter was determined by Churchill and Youngs [5]. In comparison, we have found that $W(CH_2SiMe_3)_3(\equiv CSiMe_3)$ (**1**) reacts with PMe_3, PMe_2Ph, and DMPE, forming phosphine adducts $W(CH_2SiMe_3)_3(\equiv CSiMe_3)(PR_3)$ ($PR_3 = PMe_3$, **3a**; PMe_2Ph, **3b**) (Scheme 1) and $W(CH_2SiMe_3)_3(\equiv CSiMe_3)$(DMPE-*P*) (**3e**) (Scheme 2) containing one free PMe_2 group [6]. These adducts undergo α-H migration to form their bis-alkylidene tautomers $W(CH_2SiMe_3)_2(=CHSiMe_3)_2(PR_3)$ (**4a**, **4b**) and $W(CH_2SiMe_3)_2(=CHSiMe_3)_2$(DMPE-*P*) (**4e**). The tautomeric mixtures are in equilibria, and undergo α-H abstraction to eliminate $SiMe_4$ to form, by reacting with free PR_3 and the free PMe_2 group in DMPE-*P* ligand, $W(CH_2SiMe_3)(=CHSiMe_3)(\equiv CSiMe_3)(PR_3)_2$ (**5a-b**, **6a-b**) (Scheme 1) and $W(CH_2SiMe_3)(=CHSiMe_3)(\equiv CSiMe_3)$(DMPE) (**5e**, **6e**) (Scheme 2), respectively [6].

Another example of the difference between $-CH_2SiMe_3$ and $-CH_2CMe_3$ ligands is the reactions shown in Scheme 3 [7]. $Ta(=CHR)_2(CH_2SiMe_3)(PMe_3)_2$ (R = $SiMe_3$, CMe_3) reacts with silanes to give metallocyclic products. In comparison, its neopentyl analog, $Ta(=CHCMe_3)_2(CH_2CMe_3)(PMe_3)_2$, forms unknown species with the silanes.

We have been interested in the tautomerizations between alkyl alkylidynes (**3a**, **3b**, **3e**) and bis-alkylidenes (**4a**, **4b**, **4e**) in Schemes 1 and 2 because these were among the few reported direct observation of exchanges through α-H migration [1j,m], although such exchanges had been implicated in several systems [8–12]. The tautomerization of silyl alkylidyne $(Me_3CCH_2)_2W(\equiv CCMe_3)(SiBu^tPh_2)$ with bis-alkylidene $(Me_3CCH_2)W(=CHCMe_3)_2(SiBu^tPh_2)$ was, to our knowledge, the first directly observed exchange [13].

In the current work, we studied the thermodynamics of the reversible addition of PMe_3 and PMe_2Ph to **1** forming **3a** and **3b**, respectively, in order to probe the unusual chemistry of **1** in detail. Density functional theory (DFT) studies have been performed to: (1) understand the thermodynamics and kinetics of the transformation from **1** to **4**; (2) explain why **4** is a relatively stable intermediate along the pathway to **5**.

* Corresponding authors.
E-mail addresses: zhangxh@pkusz.edu.cn (X. Zhang), chydwu@ust.hk (Y.-D. Wu), xue@ion.chem.utk.edu (Z.-L. Xue).

0277-5387/$ - see front matter © 2012 Elsevier Ltd. All rights reserved.
http://dx.doi.org/10.1016/j.poly.2012.07.042

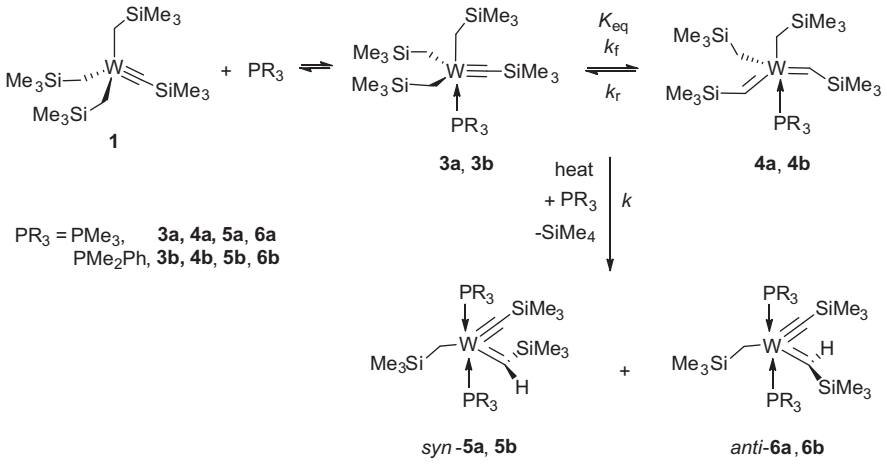

Scheme 1. Reactions of mono-dentate phosphines with **1** [6a,b,d].

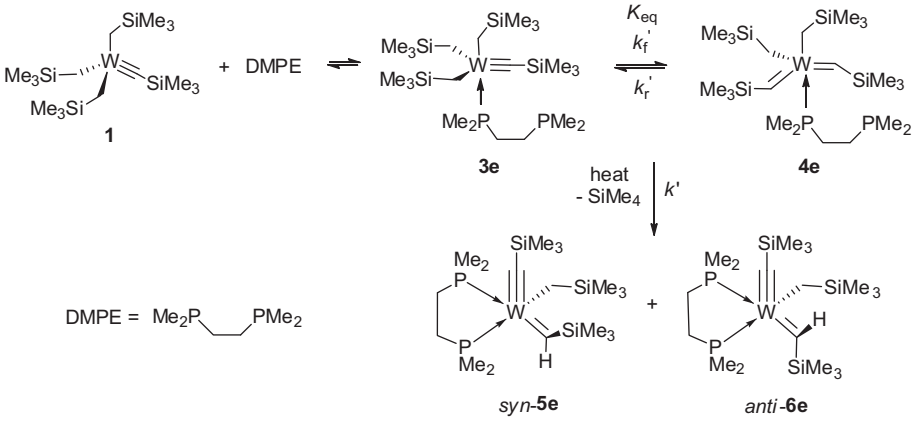

Scheme 2. Reaction of the bidentate phosphine DMPE with **1** [6c].

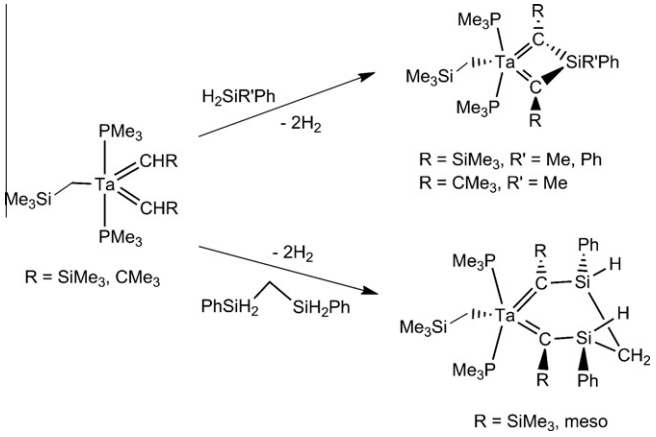

Scheme 3. Reactions of $PhR'SiH_2$ (R′ = Me, Ph, CH_2SiH_2Ph) with phosphine alkylidene complexes.

2. Material, methods and computational details

All manipulations were performed under a dry nitrogen atmosphere with the use of either a dry box or standard Schlenk techniques. Solvents were purified by distillation from potassium/benzophenone ketyl. Toluene-d_8 was dried over activated molecular sieves and stored under N_2. WCl_6 was freshly sublimed under vacuum. $W(CH_2SiMe_3)_3(\equiv CSiMe_3)$ (**1**) [3d] was prepared from $(MeO)_3WCl_3$ and six equivalents of Me_3SiCH_2MgCl by a procedure similar to that used in the preparation of $W(CH_2CMe_3)_3(\equiv CCMe_3)$ [14]. ^1H NMR spectra were recorded on a Bruker AMX-400 spectrometer.

For the thermodynamic studies, the equilibrium constants K_{eq1} were obtained from at least five separate experiments at a given temperature, and their averages are listed in Table 1. The maximum random uncertainty in the equilibrium constants were combined with the estimated systematic uncertainty of ca. 5%. The total uncertainties in the equilibrium constants were used in the $\ln K_{eq1}$ versus $1000/T$ plot in Fig. 1 and the error propagation calculations. The estimated uncertainty in the temperature measurements for an NMR probe was 1 K. The enthalpy ($\Delta H°$) and entropy ($\Delta S°$) changes were calculated from an unweighted non-linear least-squares procedure. The uncertainties in $\Delta H°$ and $\Delta S°$ were computed from the following error propagation formulas, which were derived from $-RT \ln K_{eq1} = \Delta H° - T\Delta S°$ [13].

$$(\sigma\Delta H°)^2 = \frac{R^2\left(T_{max}^2 T_{min}^4 + T_{min}^2 T_{max}^4\right)}{(T_{max} - T_{min})^4}\left[\ln\left(\frac{K_{eq1(max)}}{K_{eq1(min)}}\right)\right]^2\left(\frac{\sigma T}{T}\right)^2 + \frac{2R^2 T_{max}^2 T_{min}^2}{(T_{max} - T_{min})^2}\left(\frac{\sigma K_{eq1}}{K_{eq1}}\right)^2 \quad (1)$$

Table 1
Equilibrium constants (K_{eq1} and K'_{eq1}) of **1** + PR_3 ⇌ **3a**/**4a** and **3b**/**4b**[a].

T (K)[b]	K_{eq1}[c] for **1** + PMe_3 ⇌ **3a**/**4a**	K'_{eq1}[d] for **1** + PMe_2Ph ⇌ **3b**/**4b**
263(1)		16.4(1.5)
273(1)	$10.8(0.4) \times 10^2$	12.0(1.7)
278(1)	$7.1(0.8) \times 10^2$	
283(1)	$5.3(0.3) \times 10^2$	10.3(0.4)
288(1)	$3.6\ (0.3) \times 10^2$	
293(1)	$2.83(0.08) \times 10^2$	8.8(0.6)
298(1)	$2.23(0.03) \times 10^2$	
303(1)	$1.66(0.07) \times 10^2$	7.5(0.5)

[a] Solvent: toluene-d_8
[b] The relatively small temperature ranges of 30–40 K for the exchanges, **1** + PMe_3 ⇌ **3a**/**4a** and **1** + PMe_2Ph ⇌ **3b**/**4b**, respectively, lead to relatively large uncertainties in thermodynamic ($\Delta H°$ and $\Delta S°$) as the error calculations in the experimental section show.
[c] For the equilibrium involving PMe_3 and **3a**/**4a**, the largest random uncertainty is $\sigma K_{eq1(ran)}/K_{eq1}$ = 0.84/7.1 = 12%. The total uncertainty $\sigma K_{eq1}/K_{eq1}$ of 13% was calculated from $\sigma K_{eq1(ran)}/K_{eq1}$ = 12% and the estimated systematic uncertainty $\sigma K_{eq1(sys)}/K_{eq1}$ = 5% by $\sigma K_{eq1}/K_{eq1} = [(\sigma K_{eq1(ran)}/K_{eq1})^2 + (\sigma K_{eq1(sys)}/K_{eq1})^2]^{1/2}$.
[d] For the equilibrium involving PMe_2Ph and **3b**/**4b**, the largest random uncertainty is $\sigma K'_{eq1(ran)}/K'_{eq1}$ = 1.7/12 = 14%. The total uncertainty $\sigma K'_{eq1}/K'_{eq1}$ of 15% was calculated from $\sigma K'_{eq1(ran)}/K'_{eq1}$ = 14% and the estimated systematic uncertainty $\sigma K'_{eq1(sys)}/K'_{eq1}$ = 5% by $\sigma K'_{eq1}/K'_{eq1} = [(\sigma K'_{eq1(ran)}/K'_{eq1})^2 + (\sigma K'_{eq1(sys)}/K'_{eq1})^2]^{1/2}$.

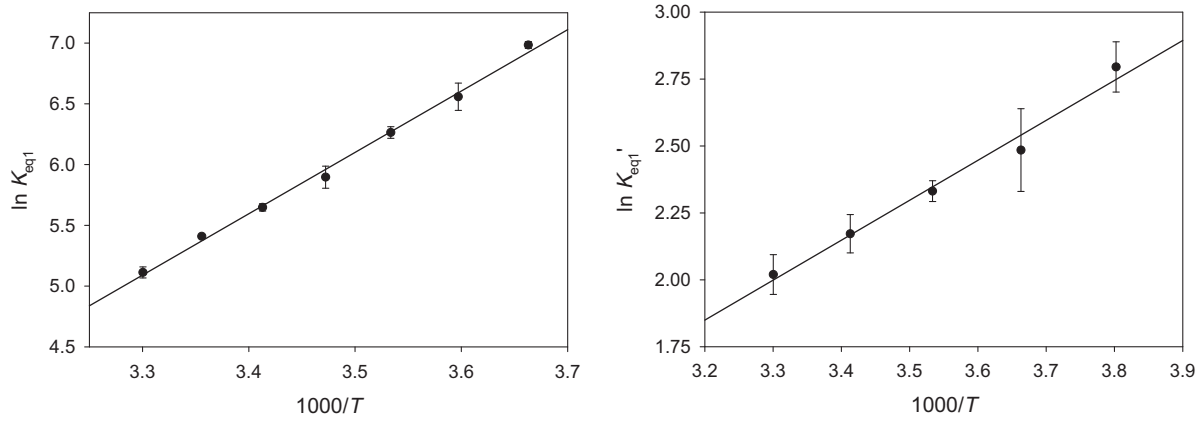

Fig. 1. Plots of ln K_{eq1} (and K'_{eq1}) vs 1000/T of the equilibria: (Left) **1** + PMe_3 ⇌ **3a**/**4a**; (Right) **1** + PMe_2Ph ⇌ **3b**/**4b**.

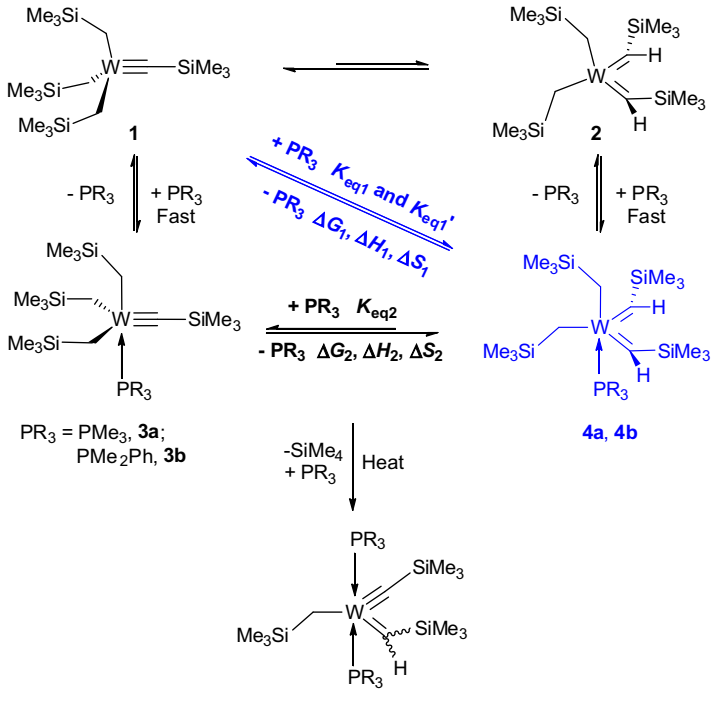

Scheme 4. Equilibria from the reactions of **1** with PR_3.

Table 2
Relative enthalpies (kcal mol^{-1}) involved in the equilibrium **1** + PMe_3 ⇌ **4a**.

Methods		1	2	3a	4a (ΔH_1)	$\Delta H_2 = H_{rel}(\mathbf{4a}) - H_{rel}(\mathbf{3a})$
Gas-phase	B3LYP	0.0	7.4	5.6	2.7	−2.9
	M06	0.0	9.2	−9.4	−12.1	−2.7
	BP86	0.0	5.8	2.6	−2.6	−5.2
Toluene	B3LYP	0.0	8.9	9.7	6.7	−3.0
	M06	0.0	7.3	−5.8	−8.8	−3.0
	BP86	0.0	9.5	6.6	2.1	−4.5
	Exp.				−10.0	−1.8

Table 3
Entropy (eu) involved in the equilibrium **1** + PMe_3 ⇌ **4a**.

Entropy		1	PMe_3	3a	4a	$\Delta S_1 = S(\mathbf{4a}) - [S(\mathbf{1}) + S(PMe_3)]$	$\Delta S_2 = S(\mathbf{4a}) - S(\mathbf{3a})$
Gas-phase	S_{Total}[a]	241.1	77.8	267.2	262.8	−56.1	−4.4
	$S_{Trans.}$	44.7	38.9	45.1	45.1		
	$S_{Rot.}$	35.9	25.4	36.4	36.4		
	$S_{Vib.}$	160.5	13.5	185.7	181.2		
Toluene	S_{total}[a]	227.2	77.2	258.7	259.4	−45.0	0.7
	$S_{trans.}$	44.7	38.9	45.1	45.1		
	$S_{rot.}$	35.7	25.3	36.5	36.4		
	$S_{vib.}$	146.7	13.0	177.2	177.9		
	$S_{corr.}$[b]	199.0	54.7	230.2	230.9	−22.8	0.7
	Exp.					−23(4)	−1.5(1.7)

[a] $S_{total} = S_{trans.} + S_{rot} + S_{vib.}$.
[b] $S_{corr.} = 0.65 \times (S_{trans.} + S_{rot.}) + S_{vib.}$.

Table 4
Reaction enthalpies (kcal mol^{-1}), entropies (eu) and Gibbs free energies (kcal mol^{-1}) for the reaction **1** + PR_3 → **4** and W—P distance of **4** (in Å).

	ΔH_1	$\Delta S_{1\text{-corr}}$[a]	$\Delta G_{1\text{-corr}}$[b]	W—P
PMe_3 (**4a**)	−8.8/−10.0	−22.8/−23	−2.0/−3.1	2.597/2.514
PMe_2Ph (**4b**)	−8.9/−3.0	−28.6/−6	−0.4/−1.2	2.609/–
PPh_3 (**4c**)	−7.4/–	−29.7/–	1.5/–	2.730/–
PCy_3 (**4d**)	−1.3/–	−29.4/–	7.5/–	2.861/–

[a] $S_{corr} = 0.65 \times (S_{trans.} + S_{rot.}) + S_{vib.}$.
[b] $\Delta G_{1\text{-Corr}} = \Delta H_1 - 298.15 \times \Delta S_{1\text{-corr.}}$.

$$(\sigma\Delta S^{\circ})^2 = \frac{2R^2T_{min}^2T_{max}^2}{(T_{max}-T_{min})^4}\left[\ln\left(\frac{K_{eq1(max)}}{K_{eq1(min)}}\right)\right]^2\left(\frac{\sigma T}{T}\right)^2 + \frac{R^2(T_{max}^2+T_{min}^2)}{(T_{max}-T_{min})^2}\left(\frac{\sigma K_{eq1}}{K_{eq1}}\right)^2 \quad (2)$$

T_{min} and T_{max} are the minimum and maximum temperatures in the current studies; T is the mean temperature in the current studies. $K_{eq1(min)}$ and $K_{eq1(max)}$ are the minimum and maximum equilibrium constants, respectively. $\sigma K_{eq1}/K_{eq1}$ is given in Table 1. Similar calculations were performed for K_{eq1}'.

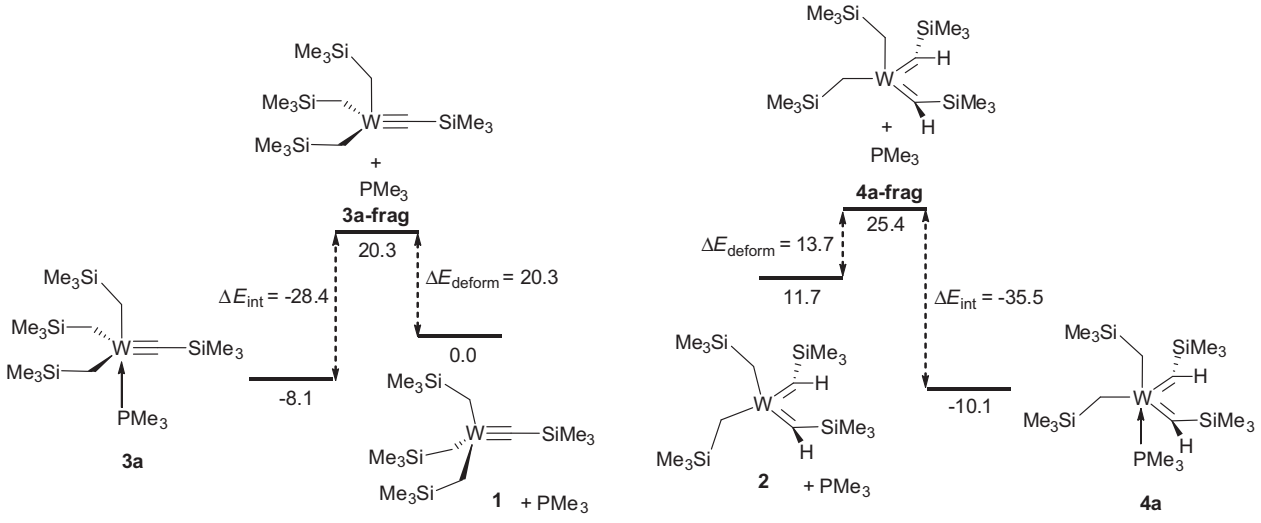

Fig. 2. Energy decomposition analysis of the binding complex **3a** and **4a** (energies in kcal mol^{-1}).

2.1. Thermodynamic study of the equilibrium between $W(CH_2SiMe_3)_3(\equiv CSiMe_3)$ (**1**), PMe_3 and the **3a** ⇌ **4a** tautomeric mixture

At least five experiments were conducted. A mixture of $W(CH_2SiMe_3)_3(\equiv CSiMe_3)$ (**1**, 20.7 mg, 0.04 mmol), 4,4′-dimethylphenyl (internal standard), and toluene-d_8 (ca. 0.65 mL) in a J.R. Youngs NMR tube was added a ca. 0.7–1.8 equiv PMe_3 *via* syringe. A weighed amount of 4,4′-dimethylphenyl was used, and its concentration in the solution was typically in the 0.02–0.03 M range. The sample was kept at room temperature for 48 h to ensure that equilibrium was established. The NMR probe was pre-cooled or pre-heated to the set temperature. After the NMR tube was inserted into the probe, a ^{1}H NMR spectrum was taken after the temperature was stabilized. K_{eq1} = [**4a**]/([**1**] [PMe_3]) were calculated from the integration of **1**, PMe_3, and **4a**. The Me peak in 4,4′-dimethylphenyl, –CH_2– peak in **1**, and the PMe_3 peak in **4a** were used in the integration and calculation of K_{eq1}.

2.2. Thermodynamic study of the equilibrium between $W(CH_2SiMe_3)_3(\equiv CSiMe_3)$ (**1**), PMe_2Ph and the **3b** ⇌ **4b** tautomeric mixture

At least three experiments were conducted. A mixture of $W(CH_2SiMe_3)_3(\equiv CSiMe_3)$ (**1**, 29.1 mg, 0.06 mmol), 4,4′-dimethylphenyl (internal standard), and toluene-d_8 (ca. 0.53 mL) in a J.R. Youngs NMR tube was added a ca. 1.0–1.5 equiv PMe_2Ph *via* syringe. A weighed amount of 4,4′-dimethylphenyl was used, and its concentration in the solution was typically in the 0.02–0.03 M range. The sample was kept at room temperature for five days to ensure that equilibrium was established. The NMR probe was pre-cooled or pre-heated to the set temperature. After the NMR tube was inserted into the probe, the ^{1}H NMR spectrum was taken after the temperature was stabilized. After the sample was placed at the set temperature for 30 min, no change in the NMR spectrum was observed. The sample was, however, kept for two hours at each temperature, during which NMR spectra were taken every 30 min to ensure no further change was observed. K_{eq1}' = [**4b**]/([**1**] [PMe_2Ph]) were calculated from the integration of **1**, PMe_2Ph, and **4b**. The Me peak in 4,4′-dimethylphenyl, –CH_2– peak in **1**, Me peak in PMe_2Ph, and the P*Me*$_2$Ph peak in **4b** were used in the integration and calculation of K_{eq1}'.

2.3. Computational methods

All calculations were carried out using Gaussian 09 [15]. The performance of the density functional theory (DFT) methods B3LYP [16,17], M06 [18], and BP86 [19] has been examined. Triple-ζ basis sets 6-311G(d, p) [20–22] were used for H, C, Si, and P; and def2-TZVP [23,24] with effective core potentials (ECP) [25] were employed for tungsten. The basis set was found to be excellent in describing metal–carbon and metal–oxygen bonds [26,27]. Geometry optimizations and vibrational frequency calculations were performed both in gas phase and solution. Solvation effects were treated with the continuum solvent models SMD [28]. Thermal corrections are calculated at standard conditions (298.15 K and 1 atm).

3. Results and discussion

3.1. Thermodynamic study of the addition of PMe_3 to **1**

Alkyl alkylidyne $W(CH_2SiMe_3)_3(\equiv CSiMe_3)$ (**1**) was treated with a various amount of PMe_3 (0.7–1.8 equiv) to probe the addition reaction of phosphine and the position of the equilibrium (Scheme 4). The addition was fast and essentially completed by the time NMR spectra were recorded. After the addition, the solution in toluene-d_8 was kept at room temperature for 48 h to ensure that equilibrium was established. Variable-temperature NMR spectra of the mixtures were studied, and the equilibrium constants, K_{eq1} = [**4a**]/([**1**] [PMe_3]), measured with a variable amount of PMe_3 between 273 and 303 K are listed in Table 1. The peaks of **3a** were very small and ignored for the calculations of K_{eq}. For the **3a** ⇌ **4a** tautomerization, **4a** dominates by a ratio of ca. 9.4–12.3 [6a,b]. A plot of ln K_{eq1} versus 1000/T (Fig. 1-Left) gave $\Delta H^\circ = -10.0$ (1.1) kcal mol^{-1} and $\Delta S^\circ = -23(4)$ eu, indicating that the addition is exothermic. The large, negative entropy of the reaction is not surprising, as in the addition, two molecules give one adduct molecule. The equilibrium constants (K_{eq1}) range from 10.8×10^2 at 273 K to 1.7×10^2 at 303 K, indicating that the **3a** ⇌ **4a** tautomers are strongly favored. Hence, PMe_3 strongly binds to **1** and its dissociation is disfavored. At higher temperatures, the equilibrium shifts towards **1** + PMe_3.

3.2. Thermodynamic study of the addition of PMe_2Ph to **1**

PMe_2Ph was utilized for comparison with PMe_3. $W(CH_2SiMe_3)_3(\equiv CSiMe_3)$ (**1**) in toluene-d_8 was added a various amount of ca. 1.0–1.5 equiv of PMe_2Ph *via* syringe. The addition to **1** is much slower than the one involving PMe_3, and takes about 2–3 days at room temperature to reach the equilibrium. The sample was kept at room temperature for 5 days to ensure that equilibrium was established.

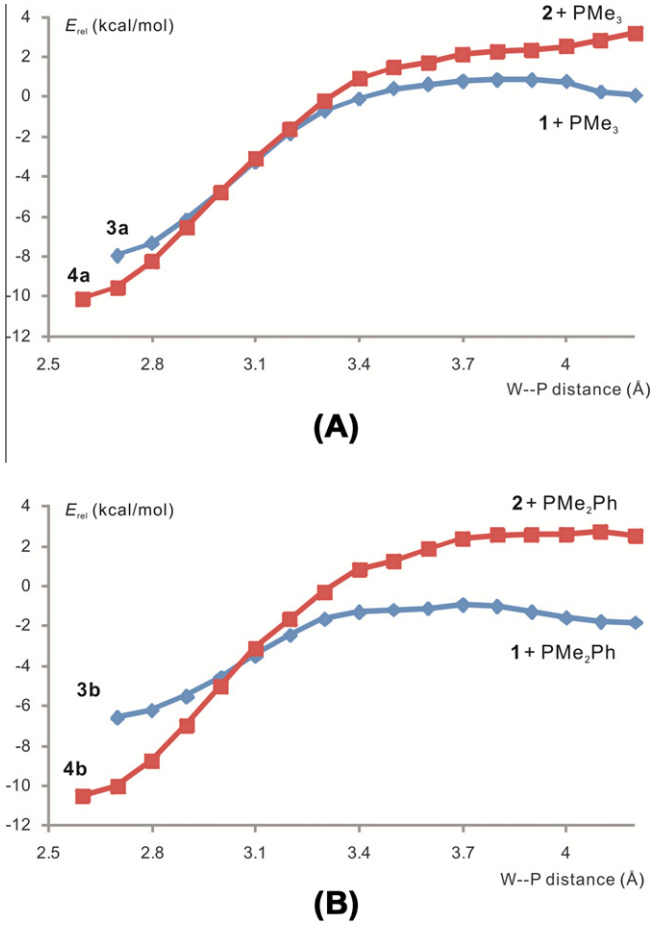

Fig. 3. Energy profile along the W—P distance.

Variable-temperature NMR spectra of the exchange of **1** and PMe_2Ph with **3b**/**4b** were studied, and the equilibrium constants, $K_{eq1}' = [\mathbf{4b}]/([\mathbf{1}]\,[PMe_2Ph])$, measured between 263 and 303 K with a variable amount of PMe_2Ph are listed in Table 1. A plot of ln K_{eq1}' versus 1000/T (Fig. 1-Right) gave $\Delta H^{o\prime} = -3.0\ (0.7)$ kcal mol^{-1} and $\Delta S^{o\prime} = -6(3)$ eu. The equilibrium constants (K_{eq1}') range from 16.4(1.5) at 263 K to 7.5(0.5) at 303 K. The much smaller equilibrium constants, in comparison to those of addition of PMe_3 to **1** (Table 1), suggest that, although the **3b** ⇌ **4b** tautomer and the bis-alkylidene (**4b**) are favored, the binding of PMe_2Ph to **1** is not as strongly favored as the binding of PMe_3. This is also reflected in smaller $\Delta H^{o\prime}$ and thus the release of much less energy during the addition of PMe_2Ph to **1**. The reaction entropy is also less negative. This is presumably due to the fact that PMe_3 is a stronger σ-donor than PMe_2Ph, and the sterics involving more bulky phenyl group versus Me in PMe_3 may also be a factor. With decreasing temperature, the equilibrium shifts towards **1**. The **1** + PMe_2Ph ⇌ **3b**/**4b** equilibrium [K_{eq1}' = 16.4(1.5) at 273 K] is shifted more to the left (**1** + PMe_2Ph) than the **1** + PMe_3 ⇌ **3a**/**4a** equilibrium [K_{eq1} = 10.8(0.4) × 10^2 at 273 K].

3.3. Calculations – benchmarking

To evaluate the performance of computational methods, the thermodynamics of two processes, the equilibrium **1** + PMe_3 ⇌ **4a** and the equilibrium **3a** ⇌ **4a**, were calculated and compared with the experimentally measured values.

Relative enthalpies calculated using a series of DFT methods are listed in Table 2. All of the relative enthalpies (ΔH_2) of the equilibrium **3a** ⇌ **4a** calculated at B3LYP, M06 and BP86 agree with the experimental measured value reasonably well [6a]. However, neither B3LYP nor BP86 level of theory can reproduce the reaction enthalpy of **1** and PMe_3 (ΔH_1). Underestimation of binding energy by various DFT methods has been reported recently [29–33]. The ΔH_1 calculated by M06 is consistent with the experimental result. The experimental results (**1** + PMe_3 ⇌ **4a**) identify M06 as an appropriate method for the system. Solvent effect does not affect the relative stabilities of **3a** and **4a** much, but decrease the binding enthalpies by ca. 4 kcal mol^{-1}.

Overestimation of the entropy for the process which involves molarity change by gas-phase calculation is well-known [34–36]. This is due to the fact that translational and rotational degrees of freedom in gas phase are reduced in solution. Several approximations have been applied to account for this effect in different systems [37–39]. As shown in Table 3, the calculated entropy loss ΔS_1 (−56.1 eu) for the bimolecular process (**1** + PMe_3 ⇌ **4a**) is significantly higher than the experimental value (−23 eu). This problem cannot be addressed by performing full optimization and frequency calculation in toluene with SMD. On the other extreme, one can estimate the entropy by neglecting the translational and rotational contribution but only taking the vibrational contribution into account [40]. However, this will underestimate the entropy simply because translation and rotation are in reality not completely suppressed. Therefore, one solution is to fit a scaling factor between 1 and 0 for the rotational and translational entropy contribution ($S_{trans.} + S_{rot.}$) to reproduce the experimental results. For the reaction studied here, a factor of 0.65 was found to be suitable for scaling the entropy in solution. The corrected entropy calculated by Eq. (3) (−22.8 eu) is closed to the experimental measured value [−23(4) eu].

$$S_{corr.} = 0.65 \times (S_{trans.} + S_{rot.}) + S_{vib.} \quad (3)$$

The M06/(6-311G(d, p), def2-TZVP with ECP) level of theory with SMD solvent corrections was chosen for the calculation in this work while the entropy values in the following discussion were corrected as outlined above.

3.4. Formation of *4*: theoretical studies of the thermodynamics

The calculated values for **1** + PMe_3 → **4a** are consistent with the measured values (Table 4). The equilibrium favors **4a**. In the case of PMe_2Ph (**4b**), the free energy is close to 0 kcal mol^{-1}, implying that the concentrations of **1** and **4** are comparable in the equilibrium mixture. The positive free energy of binding ΔG_1 and the significant longer W—P distances of **4c** and **4d** imply that such processes are unfavorable, agreeing well with the experimental observation that bulky PPh_3 and PCy_3 cannot form complexes **4**.

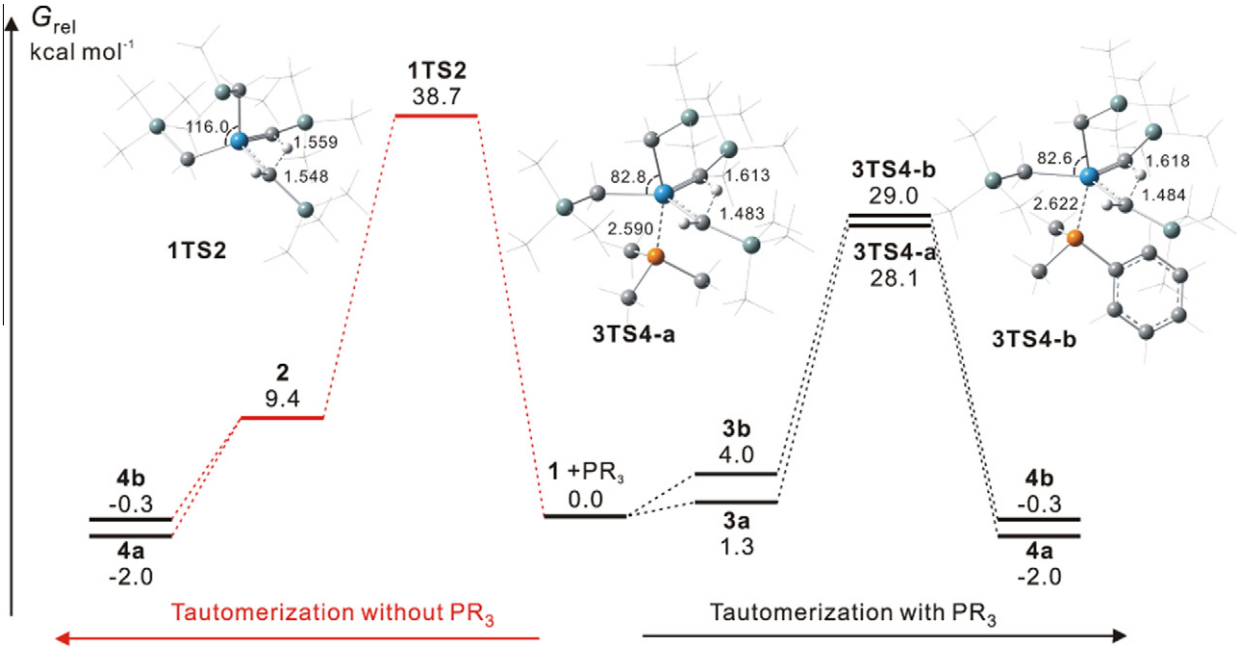

Fig. 4. Potential free energy surface for different tautomerization pathways with geometries of the transition states **1TS2**, **3TS4-a**, **3TS4-b** (distances in Å, angles in degree, free energies in kcal mol^{-1}).

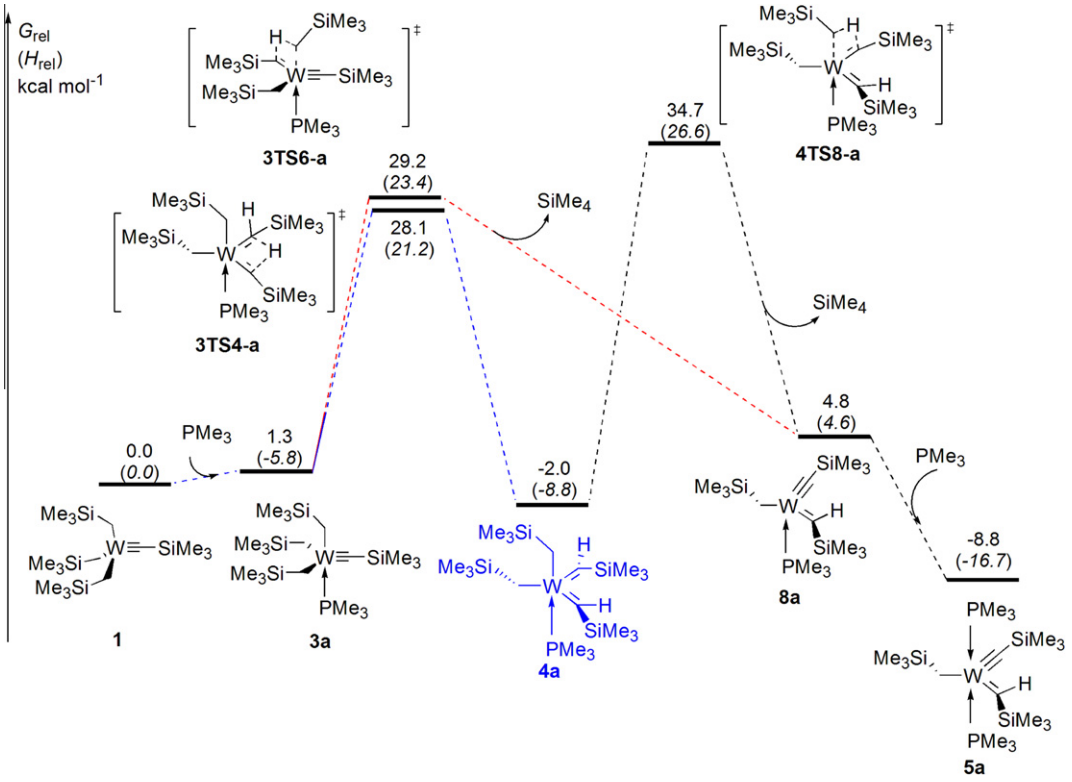

Fig. 5. Potential free energy surface for the formation of **8a** from **1** + PMe_3.

The binding preference of PR_3 ligand with the alkylidyne (**1**) or bis(alkylidene) (**2**) have already been analyzed in a molecular orbital diagram [6a]. Here, we use an energy-decomposition analysis to probe the binding energy [41,42]. This strategy decomposes the binding energy into two parts, deformation energy and interaction energy. The deformation energy is the energy induced by the distortion of binding partners into the geometries adopted in the corresponding adduct. As shown in Fig. 2, the relative energies of **3a-frag** and **4a-frag** were calculated by summating the single point energy of the tungsten fragment and the PMe_3 fragment of **3a** and **4a**, respectively. The interaction energy is the inherent energy to separate two fragments. The interaction energy of ΔE_{int} for **4a** is higher than that for **3a**, consistent with the previous MO analysis [6a]. The deformation energy for **2** is less than that of **1**, reflecting that the relative minor geometrical distortion of **2** to **4a** compared to that of **1** to **3a**.

3.5. Formation of *4*: theoretical studies of the kinetics

After discussing the thermodynamics of the formation of **4** from **1** and PR_3, we turned to the mechanism and kinetics of this process. As shown in Scheme 4, the transformation of **1** + PR_3 to **4** may undergo two possible pathways, i.e. **1** → **2** → **4** or **1** → **3** → **4**. The difference in the two pathways is a reversal of the sequence of ligand binding and tautomerization. It is hypothesized that the ligand binding is a fast step. To investigate the binding process, an energy surface scan along the W—P distance was carried out. Fig. 3 shows the relative energy (E_{rel}) versus W—P distance. The association energy curves revealed that the PR_3 binding steps are indeed barrierless.

Theoretical studies then focused on the tautomerization of the α-H transfer, which will be the rate-determining step for the formation of **4**. The structures and the free energy relative to reference (**1** + PR_3) of transition states of **1TS2**, **3TS4-a** and **3TS4-b** are shown in Fig. 4. **1TS2** adopts a tetrahedral geometry, while both of **3TS4-a** and **3TS4-b** have a trigonal bipyramidal geometry. Because the smaller distortion of **3TS4-a** and **3TS4-b** from their precursor intermediates, the free energy barriers for ligated tautomerization (**3TS4-a**: 28.1 kcal mol^{-1} and **3TS4-b**: 29.0 kcal mol^{-1}) are much lower than that of ligandless tautomerization (**1TS2**: 38.7 kcal mol^{-1}). Since the binding of PR_3 ligand is a barrierless process, it suggests that the formation of **4** undergoes the pathway along **1** → **3** → **4**, instead of **1** → **2** → **4**.

3.6. Transformation of *4* to the alkyl alkylidene alkylidyne complexes *5* and *6*

As reported previously, heating the tautomeric equilibrium mixtures of **3** ⇌ **4** in the presence of phosphines leads to the interesting tungsten alkyl alkylidene alkylidyne complexes $W(CH_2SiMe_3)(=CHSiMe_3)(\equiv CSiMe_3)(PR_3)_2$ (R_3 = Me_3, **5a**; Me_2Ph, **5b**) (Scheme 4) [6d]. The mechanism of the transformation of **4a,b** to the tungsten alkyl alkylidene alkylidyne complexes is not clear. Therefore, DFT calculations have been performed here to explore the reaction pathways. As shown in Scheme 4, the **3a** ⇌ **4a** → **5a** conversion includes two elementary steps, i.e., $SiMe_4$ elimination and binding of a second equivalent of PR_3. The previous experimental kinetics study suggests that $SiMe_4$ elimination occurs prior to the addition of a second PR_3. That allows us to focus on the step of $SiMe_4$ elimination.

The potential energy surface of the formation of **8a**, which then binds PMe_3 to give the bisphosphine product **5a**, from **1** is shown in Fig. 5. The coordination of the phosphine ligand PMe_3 and the equilibrium between **3a** and **4a** have been discussed above. **4a** is a thermodynamically stable intermediate. At higher temperatures, **3a** and **4a** may undergo an α-H abstraction to eliminate $SiMe_4$ and give the monophosphine and alkyl alkylidene alkylidyne intermediate **8a**. For **3TS6-a**, the α-H transfer takes place from one alkyl group to another alkyl group, while the α-H transfer occurs from alkylidene to alkyl group in **4TS6-a**. The relative free energy of

4TS6-a is 34.7 kcal mol^{-1}, 5.5 kcal mol^{-1} higher than **3TS6-a**, suggesting that the pathway **4a** → **3a** → **8a** is more favorable for the formation of the tungsten alkyl alkylidene alkylidyne complex **5a**. The overall enthalpy and free energy barrier from **4a** to **8a** are calculated to be 32.2 and 31.2 kcal mol^{-1}, in a reasonable agreement with the experimental measured values (29 and 28 kcal mol^{-1}). The slightly higher barrier of transformation from **4a** to **8a** than that of the transformation from **1** to **4a**, indicating that **4a** is a kinetically stable intermediate.

4. Concluding remarks

Addition of two mono-dentate phosphines (PR_3 = PMe_3 and PMe_2Ph) to $W(CH_2SiMe_3)_3(\equiv CSiMe_3)$ (**1**), forming $W(CH_2SiMe_3)_3(\equiv CSiMe_3)(PR_3)$ (**3a**, **3b**) and their bis-alkylidene tautomers $W(CH_2SiMe_3)_2(=CHSiMe_3)_2(PR_3)$ (**4a**, **4b**), has been found to be reversible. It should be noted that the reaction of excess $W(CH_2SiMe_3)_3(\equiv CSiMe_3)$ (**1**) and $Me_2PCH_2CH_2PMe_2$ (DMPE) appears to be more complicated than the reaction of **1** with the mono-dentate phosphines, and is not pursued in the current work. Using a comparison with the experimental thermodynamic data, benchmarking work has been carried out and M06 is found to be an appropriate method for this system. Consequently, a detailed computational study has been performed to investigate the reaction of $W(CH_2SiMe_3)_3(\equiv CSiMe_3)$ (**1**) with PR_3. Because the binding of PR_3 ligand is barrierless and the PR_3 facilitates the α-H migration, the formation of **4** undergoes the pathway along **1** → **3** → **4**, instead of **1** → **2** → **4**. Heating the tautomeric equilibrium mixtures of **3** ⇌ **4** in the presence of the phosphine gives the tungsten alkyl alkylidene alkylidyne complexes $W(CH_2SiMe_3)(=CHSiMe_3)(\equiv CSiMe_3)(PR_3)_2$ (PR_3 = PMe_3, **5a**; PMe_2Ph, **5b**). The potential energy surface of the formation of **8a** indicates that the relative free energy of **4TS6-a** is higher than **3TS6-a**. This suggests the formation of **8a** along the pathway **4a** → **3a** → **8a**, followed by binding of **8a** to PMe_3 to give the bisphosphine product **5a**. This study provides a missing piece to understand the role of **4** plays along the pathway of the reaction of **1** and PR_3. **4** is found to be a thermodynamically and kinetically stable intermediate.

Acknowledgments

Financial support from the National Science Foundation of China (21133002), US National Science Foundation (CHE-1012173), the Shenzhen Peacock Program, and Peking University Shenzhen Graduate School is acknowledged. We would like to thank Prof. Olaf Wiest for helpful discussion and the Shenzhen Supercomputer Center for computational resources.

References

[1] See, e.g., the following reviews and references therein: (a) R.R. Schrock, Chem. Rev. 102 (2002) 145;
(b) R.H. Grubbs, Tetrahedron 60 (2004) 7117;
(c) R.R. Schrock, Chem. Rev. 109 (2009) 3211;
(d) X. Wu, M. Tamm, Beilstein J. Org. Chem. 7 (2011) 82;
(e) M.C. Haibach, S. Kundu, M. Brookhart, A.S. Goldman, Acc. Chem. Res. 45 (2012) 947;
(f) K. Nomura, J. Chin. Chem. Soc. 59 (2012) 139;
(g) F. Rascon, C. Coperet, J. Organomet. Chem. 696 (2011) 4121;
(h) R.R. Schrock, Dalton Trans. 40 (2011) 7484;
(i) A.L. Odom, Dalton Trans. 40 (2011) 2689;
(j) Z.-L. Xue, L.A. Morton, J. Organomet. Chem. 696 (2011) 3924;
(k) D.J. Mindiola, Acc. Chem. Res. 39 (2006) 813;
(l) R.E. Da Re, M.D. Hopkins, Coord. Chem. Rev. 249 (2005) 1396;
(m) X. Yu, L.A. Morton, Z.-L. Xue, Organometallics 23 (2004) 2210;
(n) J. Feldman, R.R. Schrock, Prog. Inorg. Chem. 39 (1991) 1;
(o) A. Mayr, H. Hoffmeister, Adv. Organomet. Chem. 32 (1991) 227;
(p) W.A. Nugent, J.M. Mayer, Metal-Ligand Multiple Bonds, Wiley, New York, 1988.

[2] See, e.g., the following recent papers: (a) S. Sarkar, K.P. McGowan, S. Kuppuswamy, I. Ghiviriga, K.A. Abboud, A.S. Veige, J. Am. Chem. Soc. 134 (2012) 4509;
(b) A.M. Geyer, M.J. Holland, R.L. Gdula, J.E. Goodman, M.J.A. Johnson, J.W. Kampf, J. Organomet. Chem. 708–709 (2012) 1;
(c) J. Heppekausen, R. Stade, R. Goddard, A. Fuerstner, J. Am. Chem. Soc. 134 (2012) 11045;
(d) J.G. Andino, H. Fan, A.R. Fout, B.C. Bailey, M.-H. Baik, D.J. Mindiola, J. Organomet. Chem. 696 (2011) 4138;
(e) S. Aguado-Ullate, J.J. Carbo, O. Gonzalez-del Moral, A. Martin, M. Mena, J.-M. Poblet, C. Santamaria, Inorg. Chem. 50 (2011) 6269;
(f) X. Wu, C.G. Daniliuc, C.G. Hrib, M. Tamm, J. Organomet. Chem. 696 (2011) 4147;
(g) B.A. Dougan, Z.-L. Xue, Sci. China Chem. 54 (2011) 1903;
(h) D. Zhang, Y. Zhang, K. Gao, C.-S. Wang, Chin. J. Inorg. Chem. 24 (2008) 861;
(i) S. Chen, M.H. Chisholm, Inorg. Chem. 48 (2009) 10358;
(j) X. Solans-Monfort, C. Coperet, O. Eisenstein, J. Am. Chem. Soc. 132 (2010) 7750;
(k) M. Yu, I. Ibrahem, M. Hasegawa, R.R. Schrock, A.H. Hoveyda, J. Am. Chem. Soc. 134 (2012) 2788;
(l) J. Zhu, G. Jia, Z. Lin, Organometallics 25 (2006) 1812;
(m) B.C. Bailey, R.R. Schrock, S. Kundu, A.S. Goldman, Z. Huang, M. Brookhart, Organometallics 28 (2009) 355;
(n) W. Zhang, J. Yamada, K. Nomura, Organometallics 27 (2008) 5353;
(o) N. Merle, J. Trebosc, A. Baudouin, I.D. Rosal, L. Maron, K. Szeto, M. Genelot, A. Mortreux, M. Taoufik, L. Delevoye, J. Am. Chem. Soc. 134 (2012) 9263;
(p) Y.P. Barinova, Y.E. Begantsova, N.E. Stolyarova, I.K. Grigorieva, A.V. Cherkasov, G.K. Fukin, Y.A. Kurskii, L.N. Bochkarev, G.A. Abakumov, Inorg. Chim. Acta 363 (2010) 2313.

[3] (a) R.R. Schrock, J.D. Fellmann, J. Am. Chem. Soc. 100 (1978) 3359;
(b) D.N. Clark, R.R. Schrock, J. Am. Chem. Soc. 100 (1978) 6774;
(c) W. Mowat, G. Wilkinson, J. Chem. Soc., Dalton Trans. (1973) 1120;
(d) R.A. Andersen, M.H. Chisholm, J.F. Gibson, W.W. Reichert, I.P. Rothwell, G. Wilkinson, Inorg. Chem. 20 (1981) 3934;
(e) L.-T. Li, M. Hung, Z.-L. Xue, J. Am. Chem. Soc. 117 (1995) 12746;
(f) J.K.C. Abbott, L.-T. Li, Z.-L. Xue, J. Am. Chem. Soc. 131 (2009) 8246.

[4] (a) Z.-L. Xue, L.-T. Li, L.K. Hoyt, J.B. Diminnie, J.L. Pollitte, J. Am. Chem. Soc. 116 (1994) 2169;
(b) Y.-D. Wu, K.W.K. Chan, Z.-L. Xue, J. Am. Chem. Soc. 117 (1995) 9259;
(c) L.-T. Li, Z.-L. Xue, G.P.A. Yap, A.L. Rheingold, Organometallics 14 (1995) 4992;
(d) L.-T. Li, J.B. Diminnie, X.-Z. Liu, J.L. Pollitte, Z.-L. Xue, Organometallics 15 (1996) 3520;
(e) J.B. Diminnie, H.D. Hall, Z.-L. Xue, Chem. Comm. (1996) 2383;
(f) X.-Z. Liu, L.-T. Li, J.B. Diminnie, G.P.A. Yap, A.L. Rheingold, Z.-L. Xue, Organometallics 17 (1998) 4597.

[5] M.R. Churchill, W.J. Youngs, Inorg. Chem. 18 (1979) 2454.

[6] (a) L.A. Morton, X.-H. Zhang, R. Wang, Z. Lin, Y.-D. Wu, Z.-L. Xue, J. Am. Chem. Soc. 126 (2004) 10208;
(b) L.A. Morton, R. Wang, X. Yu, C.F. Campana, I.A. Guzei, G.P.A. Yap, Z.-L. Xue, Organometallics 25 (2006) 427;
(c) B.A. Dougan, Z.-L. Xue, Organometallics 28 (2009) 1295;
(d) L.A. Morton, S. Chen, H. Qiu, Z.-L. Xue, J. Am. Chem. Soc. 129 (2007) 7277.

[7] (a) J.B. Diminnie, Z.-L. Xue, J. Am. Chem. Soc. 119 (1997) 12657;
(b) J.B. Diminnie, J.R. Blanton, H. Cai, K.T. Quisenberry, Z.-L. Xue, Organometallics 20 (2001) 1504;
(c) J.R. Blanton, T.-N. Chen, J.B. Diminnie, H. Cai, Z.-Z. Wu, L.-T. Li, K.R. Sorasaenee, K.T. Quisenberry, H.-J. Pan, C.-S. Wang, S.-H. Choi, Y.-D. Wu, Z.-Y. Lin, I.A. Guzei, A.L. Rheingold, Z.-L. Xue, J. Mol. Catal. A 190 (2002) 101;
(d) J.B. Diminnie, X.-Z. Liu, H. Cai, Z.-Z. Wu, J.R. Blanton, A.A. Tuinman, K.T. Quisenberry, C.E. Vallet, R.A. Zuhr, D.B. Beach, Z.-H. Peng, Y.-D. Wu, T.E. Concolino, A.L. Rheingold, Z.-L. Xue, Pure Appl. Chem. 73 (2001) 331.

[8] A.M. LaPointe, R.R. Schrock, W.M. Davis, J. Am. Chem. Soc. 117 (1995) 4802.

[9] K.G. Caulton, M.H. Chisholm, W.E. Streib, Z.-L. Xue, J. Am. Chem. Soc. 113 (1991) 6082.

[10] Z.-L. Xue, K.G. Caulton, M.H. Chisholm, Chem. Mater. 3 (1991) 384.

[11] Z.-L. Xue, S.-H. Chuang, K.G. Caulton, M.H. Chisholm, Chem. Mater. 10 (1998) 2365.

[12] K.G. Caulton, R.H. Cayton, M.H. Chisholm, J.C. Huffman, E.B. Lobkovsky, Z.-L. Xue, Organometallics 11 (1992) 321.

[13] (a) T.-N. Chen, Z.-Z. Wu, L.-T. Li, K.R. Sorasaenee, J.B. Diminnie, H.-J. Pan, I.A. Guzei, A.L. Rheingold, Z.-L. Xue, J. Am. Chem. Soc. 120 (1998) 13519;
(b) T.-N. Chen, X.-H. Zhang, C.-S. Wang, S.-J. Chen, Z.-Z. Wu, L.-T. Li, K.R. Sorasaenee, J.B. Diminnie, H.-J. Pan, I.A. Guzei, A.L. Rheingold, Y.-D. Wu, Z.-L. Xue, Organometallics 24 (2005) 1214.

[14] R.R. Schrock, J. Sancho, S.F. Pederson, Inorg. Synth. 26 (1989) 45.

[15] M.J. Frisch, G.W. Trucks, H.B. Schlegel, G.E. Scuseria, M.A. Robb, J.R. Cheeseman, G. Scalmani, V. Barone, B. Mennucci, G.A. Petersson, H. Nakatsuji, M. Caricato, X. Li, H.P. Hratchian, A.F. Izmaylov, J. Bloino, G. Zheng, J.L. Sonnenberg, M. Hada, M. Ehara, K. Toyota, R. Fukuda, J. Hasegawa, M. Ishida, T. Nakajima, Y. Honda, O. Kitao, H. Nakai, T. Vreven, J.A. Montgomery Jr., J.E. Peralta, F. Ogliaro, M. Bearpark, J.J. Heyd, E. Brothers, K.N. Kudin, V.N. Staroverov, R. Kobayashi, J. Normand, K. Raghavachari, A. Rendell, J.C. Burant, S.S. Iyengar, J. Tomasi, M. Cossi, N. Rega, N.J. Millam, M. Klene, J.E. Knox, J.B. Cross, V. Bakken, C. Adamo, J. Jaramillo, R. Gomperts, R.E. Stratmann, O. Yazyev, A.J. Austin, R. Cammi, C.

Pomelli, J.W. Ochterski, R.L. Martin, K. Morokuma, V.G. Zakrzewski, G.A. Voth, P. Salvador, J.J. Dannenberg, S. Dapprich, A.D. Daniels, Ö. Farkas, J.B. Foresman, J.V. Ortiz, J. Cioslowski, D.J. Fox, Gaussian 09, Revision A.1, Gaussian, Inc., Wallingford, CT, 2009.
[16] A.D. Becke, J. Chem. Phys. 98 (1993) 5648.
[17] C. Lee, W. Yang, R.G. Parr, Phys. Rev. B 37 (1988) 785.
[18] Y. Zhao, D.G. Truhlar, Theor. Chem. Acc. 120 (2008) 215.
[19] J.P. Perdew, Phys. Rev. B 33 (1986) 8822.
[20] A.D. McLean, G.S. Chandler, J. Chem. Phys. 72 (1980) 5639.
[21] K. Raghavachari, J.S. Binkley, R. Seeger, J.A. Pople, J. Chem. Phys. 72 (1980) 650.
[22] R.C. Binning Jr., L.A. Curtiss, J. Comp. Chem. 11 (1990) 1206.
[23] F. Weigend, R. Ahlrichs, Phys. Chem. Chem. Phys. 7 (2005) 3297.
[24] (a) The basis sets were obtained from the Gaussian Basis Set Library EMSL at https://bse.pnl.gov/bse/portal.;
(b) D. Feller, J. Comput. Chem. 17 (1996) 1571;
(c) K.L. Schuchardt, B.T. Didier, T. Elsethagen, L. Sun, V. Gurumoorthi, J. Chase, J. Li, T.L. Windus, J. Chem. Inf. Model 47 (2007) 1045.
[25] B. Metz, H. Stoll, M. Dolg, J. Chem. Phys. 113 (2000) 2563.
[26] X. Zhang, H. Schwarz, Chem. Eur. J. 16 (2010) 5882.
[27] X. Zhang, H. Schwarz, Theor. Chem. Acc. 129 (2011) 389.
[28] A.V. Marenich, C.J. Cramer, D.G. Truhlar, J. Phys. Chem. B 113 (2009) 6378.
[29] Y. Zhao, D.G. Truhlar, Acc. Chem. Res. 41 (2008) 157.
[30] Y. Zhao, D.G. Truhlar, Org. Lett. 9 (2007) 1967.
[31] Y. Zhao, D.G. Truhlar, J. Chem. Theor. Comput. 5 (2009) 324.
[32] H.-C. Yang, Y.-C. Huang, Y.-K. Lan, T.-Y. Luh, Y. Zhao, D.G. Truhlar, Organometallics 30 (2011) 4196.
[33] Y. Zhao, D.G. Truhlar, Chem. Phys. Lett. 502 (2011) 1.
[34] D.H. Wertz, J. Am. Chem. Soc. 102 (1980) 5316.
[35] B.O. Leung, D.L. Reid, D.A. Armstrong, A. Rauk, J. Phys. Chem. A 108 (2004) 2720.
[36] D. Ardura, R. López, T.L. Sordo, J. Phys. Chem. B 109 (2005) 23618.
[37] J. Cooper, T. Ziegler, Inorg. Chem. 41 (2002) 6614.
[38] P.A. Dub, R. Poli, J. Mol. Catal. A 324 (2010) 89.
[39] M. Wang, T. Fan, Z. Lin, Organometallics 31 (2012) 560.
[40] M. Sumimoto, N. Iwane, T. Takahama, S. Sakaki, J. Am. Chem. Soc. 126 (2004) 10457.
[41] T. Ziegler, A. Rauk, Theor. Chim. Acta 46 (1977) 1.
[42] K. Morokuma, Acc. Chem. Res. 10 (1977) 294.

Please cite this article in press as: P. Chen et al., Polyhedron (2012), http://dx.doi.org/10.1016/j.poly.2012.07.042